Supplement of Atmos. Chem. Phys., 24, 1415–1427, 2024
https://doi.org/10.5194/acp-24-1415-2024-supplement

Atmospheric Chemistry and Physics
Open Access

Supplement of

Estimation of the atmospheric hydroxyl radical oxidative capacity using multiple hydrofluorocarbons (HFCs)

Rona L. Thompson et al.

Correspondence to: Rona L. Thompson (rlt@nilu.no)

Supplementary Tables

Table S1: Arrhenius rate constants for the five HFCs used in this study

Species	**A**	**B**	**Reference**
HFC-134a	1.5×10^{-12}	1750	(Wilson, et al., 2007)
HFC-152a	2.4×10^{-12}	1260	(Wilson, et al., 2007)
HFC-365mfc	1.68×10^{-12}	1585	(Mellouki et al., 1995)
HFC-245fa	6.32×10^{-13}	1331	(Orkin et al., 1996)
HFC-32	1.9×10^{-12}	1550	(Wilson, et al., 2007)

Table S2: Sites used for the calculation of the mean for each latitudinal band. The species HFC-134a, HFC-152a, HFC-365mfc and HFC-32 are measured at all sites, but HFC-245fa is only measured at AGAGE sites. Note that the additional sites in the NOAA network, Harvard Forest, US (HFM) and Park Falls, US (LEF) were not included as observations at these sites are sensitive to local emissions and less representative of the well-mixed background. The altitude is given in metres above sea level.

Site	**Full name**	**Latitude**	**Longitude**	**Altitude**	**Network(s)**
Box 1: 90°-30°N					
ALT	Alert, Canada	82.45	-62.51	195	NOAA
BRW	Barrow, Alaska, US	71.32	-156.60	28	NOAA, Archive
MHD	Mace Head, Ireland	53.33	-9.90	26	NOAA, AGAGE
NWR	Niwot Ridge, US	40.05	-105.63	3526	NOAA
SUM	Summit, Greenland	72.6	-38.4	3200	NOAA
THD	Trinidad Head, US	41.03	-124.15	112	NOAA, AGAGE, Archive
GSN	Gosan, Korea	33.28	127.17	72	AGAGE
JFJ	Jungfraujoch, Switzerland	46.55	7.99	3580	AGAGE
CMN	Monte Cimone, Italy	44.17	10.68	2165	AGAGE
ZEP	Zeppelin, Svalbard, Norway	78.91	11.88	474	AGAGE
LJA	La Jolla, California, US	32.82	-117.27	5	Archive
Box 2: 30°N-0°					
KUM	Cape Kumukahi, Hawaii, US	19.52	-154.82	8	NOAA
MLO	Mauna Loa, Hawaii, US	19.53	-155.58	3437	NOAA
RPB	Barbados	13.17	-59.43	45	AGAGE
Box 3: 0°-30°S					
SMO	American Samoa	-14.25	-170.57	60	NOAA, AGAGE
Box 4: 30°-90°S					
CGO	Cape Grim, Australia	-40.68	144.68	164	NOAA, AGAGE, Archive
PSA	Palmer Station, Antarctica	-64.60	-64.0	10	NOAA
SPO	South Pole, Antarctica	-89.98	-24.80	2821	NOAA

Table S3: Start of the atmospheric record (within the inversion period 2000-2021) for each site in the NOAA and AGAGE networks and the Archive data.

Network	Site	HFC-134a	HFC-152a	HFC-365mfc	HFC-245fa	HFC-32
NOAA	ALT	2000.1	2000.6	2009.6	NA	2014.8
	BRW	2000.1	2000.7	2009.7	NA	2009.3
	CGO	2000.1	2000.6	2009.7	NA	2009.3
	KUM	2000.1	2000.7	2009.7	NA	2009.3
	MHD	2001.4	2001.4	2009.7	NA	2015.0
	MLO	2000.1	2000.7	2009.7	NA	2009.3
	NWR	2000.1	2000.7	2009.7	NA	2014.9
	PSA	2000.1	2000.4	2009.3	NA	2014.6
	SMO	2000.1	2000.7	2009.6	NA	2009.3
	SPO	2000.1	2000.1	2009.2	NA	2008.8
	SUM	2004.5	2004.5	2009.5	NA	2014.8
	THD	2002.2	2002.2	2009.7	NA	2009.3
AGAGE	RPB	2005.4	2005.4	2006.4	2008.0	2005.4
	GSN	2007.9	2007.9	NA	NA	NA
	JFJ	2000.1	2000.1	2008.3	2004.7	2008.3
	MHD	2000.1	2000.1	2005.1	2006.9	2005.1
	CMN	2002.1	2002.1	NA	NA	NA
	SMO	2006.4	2006.4	2006.4	2007.9	2006.4
	CGO	2000.1	2000.1	2005.4	2006.5	2005.1
	THD	2005.3	2005.3	2005.4	2008.0	2005.3
	ZEP	2001.1	2001.1	2010.8	2010.8	2010.8
ARCHIVE	90°-30°N	NA	NA	2000.3	2000.3	NA
	30°-90°S	NA	NA	2000.3	2000.3	NA

Table S4: Calibration scales for each species and network

Species	AGAGE	NOAA
HFC-134a	SIO-05	NOAA-1995
HFC-152a	SIO-05	NOAA-2004
HFC-365mfc	SIO-14	NOAA-2011
HFC-245fa	SIO-14	N/A
HFC-32	SIO-07	NOAA-2016

Table S5: Annual mean OH anomalies (%) from the mean estimates for inversions using i) adjustments made to the AGAGE data to match NOAA, ii) adjustments made to NOAA data to match AGAGE, and iii) inversions that included the very short-lived species HFC-152a and HFC-32.

Year	**adjusted AGAGE**	**adjusted NOAA**	**incl. HFC-32 & HFC-152a**
2004	0.04	0.12	0.26
2005	-0.54	-0.49	-0.61
2006	-0.40	-0.39	-0.17
2007	-0.43	-0.40	-0.10
2008	-0.64	-0.59	-0.77
2009	1.05	1.03	1.40
2010	0.70	0.78	0.82
2011	0.07	0.18	0.14
2012	0.13	0.22	0.32
2013	0.58	0.60	0.79
2014	0.54	0.55	0.78
2015	-0.18	-0.17	-0.19
2016	-0.44	-0.53	-0.40
2017	-0.36	-0.54	-0.46
2018	-1.09	-1.23	-1.57
2019	-0.41	-0.65	-1.05
2020	-0.30	-0.51	-1.63
2021	0.43	0.36	-0.16

Table S6: Sites in the NOAA discrete sampling network used for the calculation of the mean CH_4 mole fraction in each latitudinal band. The altitude is given in metres above sea level.

Site	Full name	Latitude	Longitude	Altitude
Box 1: 90°-30°N				
ALT	Alert, Canada	82.45	-62.51	185
ZEP	Zeppelin, Swalbard, Norway	78.91	11.89	474
SUM	Summit, Greenland	72.60	-38.42	3209.54
BRW	Barrow, Alaska, US	71.32	-156.61	11
PAL	Pallas, Finland	67.97	24.12	565
ICE	Iceland	63.40	-20.29	118
CBA	Cold Bay, Alaska, US	55.21	-162.72	21.34
MHD	Mace Head, Ireland	53.33	-9.90	5
SHM	Shemya Island, Alaska, US	52.71	174.13	23
HUN	Hegyhatsal, Hungary	46.95	16.65	248
UUM	Ulaan Uul, Mongolia	44.45	111.10	1007
THD	Trinidad Head, CA, US	41.05	-124.15	107
NWR	Niwot Ridge, CO, US	40.05	-105.59	3523
UTA	Wendover, Utah, US	39.90	-113.72	1327
AZR	Azores, Portugal	38.77	-27.38	19
TAP	Tae-ahn Peninsula, Korea	36.74	126.13	16
WLG	Mt Waliguan, China	36.29	100.90	3810
BMW	Tudor Hill, Bermuda, UK	32.26	-64.88	30
Box 2: 30°N-0°				
WIS	Weizman Institute of Science, Israel	29.96	35.06	151
IZO	Izana, Tenerife, Spain	28.31	-16.50	2372.9
MID	Midway Island, US	28.22	-177.37	4.6
KEY	Key Biscayne, FO, US	25.67	-80.16	1
ASK	Assekrem, Algeria	23.26	5.63	2710
KUM	Cape Kumukahi, Hawaii, US	19.56	-154.89	8
MLO	Mauna Loa, Hawaii, US	19.54	-155.58	3397
GMI	Mariana Islands, Guam	13.39	144.66	0
RPB	Ragged Point, Barbados	13.17	-59.43	15
CHR	Christmas Island, Kiribati	1.70	-157.15	0
Box 3: 0°-30°S				
SEY	Mahi, Seychelles	-4.68	55.53	2
ASC	Ascension Island, UK	-7.97	-14.40	85
SMO	American Samoa	-14.25	-170.56	42
NMB	Gobabeb, Namibia	-23.58	15.03	456
EIC	Easter Island	-27.16	-109.43	47

Table S6. Continued

Box 3: 30°-90°S				
CPT	Cape Point, South Africa	-34.35	18.49	230
CGO	Cape Grim, Australia	-40.68	144.69	94
BHD	Baring Head, New Zealand	-41.41	174.87	85
CRZ	Crozet Island, France	-46.43	51.85	197
USH	Ushuaia, Argentina	-54.85	-68.31	12
PSA	Palmer Station, Antartica, US	-64.77	-64.05	10
SYO	Syowa Station, Antarctica, Japan	-69.01	39.59	14
HBA	Halley Station, Antarctica, UK	-75.61	-26.21	30
SPO	South Pole, Antarctica, US	-89.98	-24.80	2810

Supplementary Figures

Figure S1: Comparison of the AGAGE and NOAA measurements of HFC-32 (upper panel) and HFC-365mfc (lower panel) before and after adjustment. In each panel the top row shows the unadjusted and adjusted NOAA observations and the AGAGE observations, and the lower panel shows the difference between NOAA and AGAGE with and without adjustment. The adjustment was calculated as a quadratic function fit to the differences between the NOAA and AGAGE records.

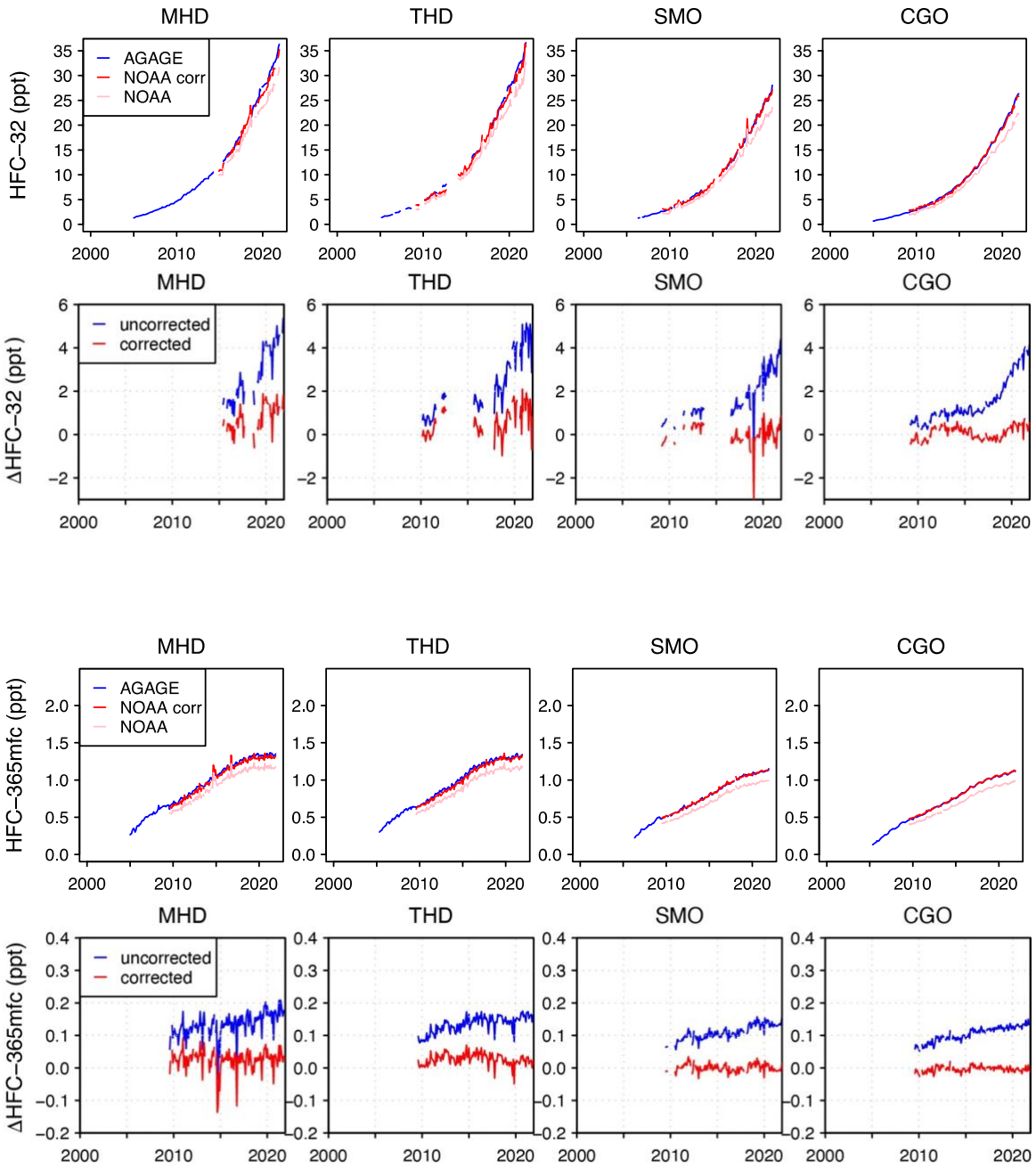

Figure S2: Monthly mean mole fractions in each latitudinal box in the lower troposphere calculated as the mean of all sites in each box: a) HFC-134a, b) HFC-152a, c) HFC-365mfc, d) HFC-245fa, and e) HFC-32. These are the observation data that were assimilated in the inversions.

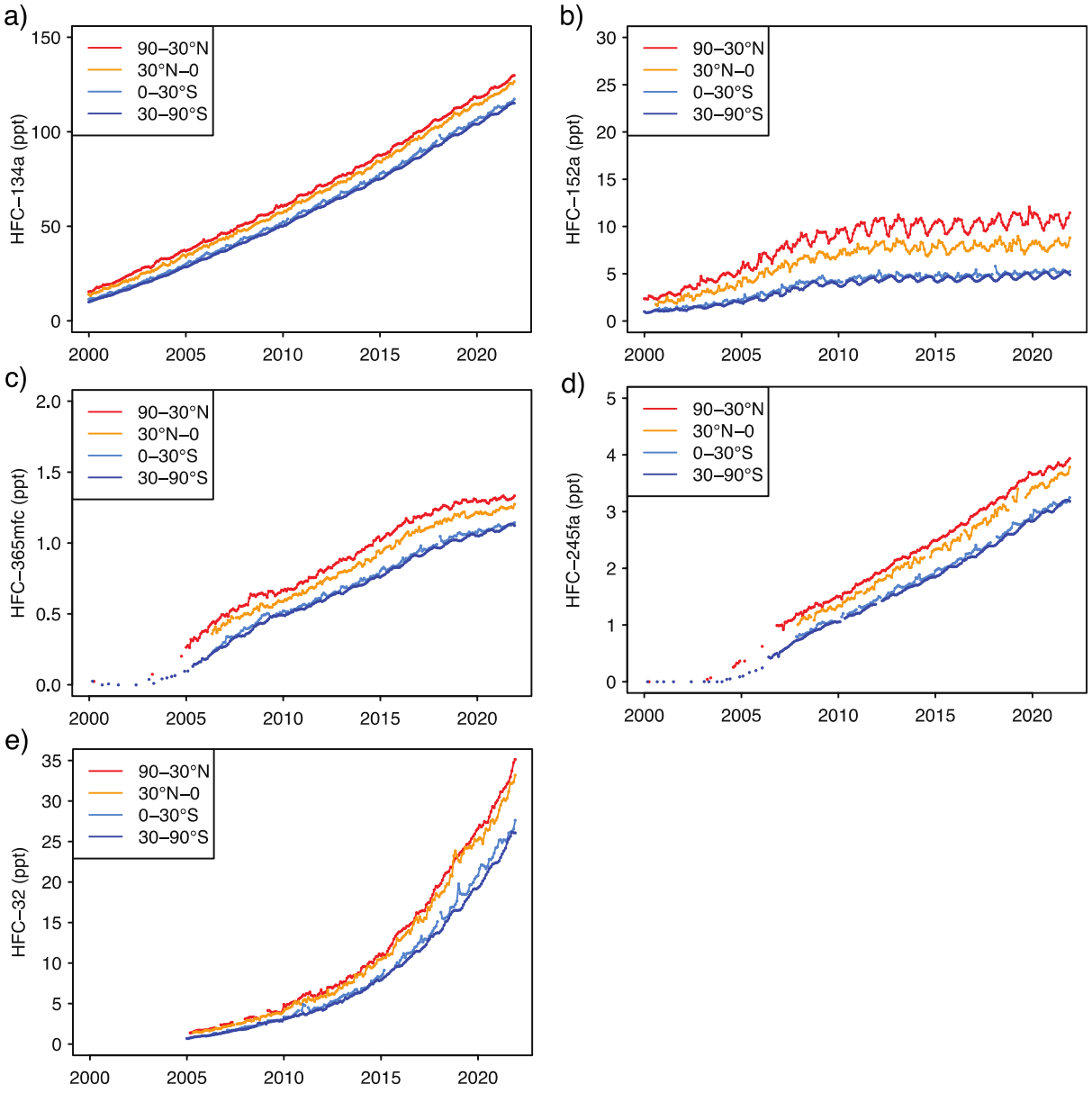

Figure S3: Dependence of the posterior emissions (top) and OH (bottom) on the choice of uncertainty. Results are shown for the inversion using HFC-134a, HFC-152a, and HFC-365mfc.

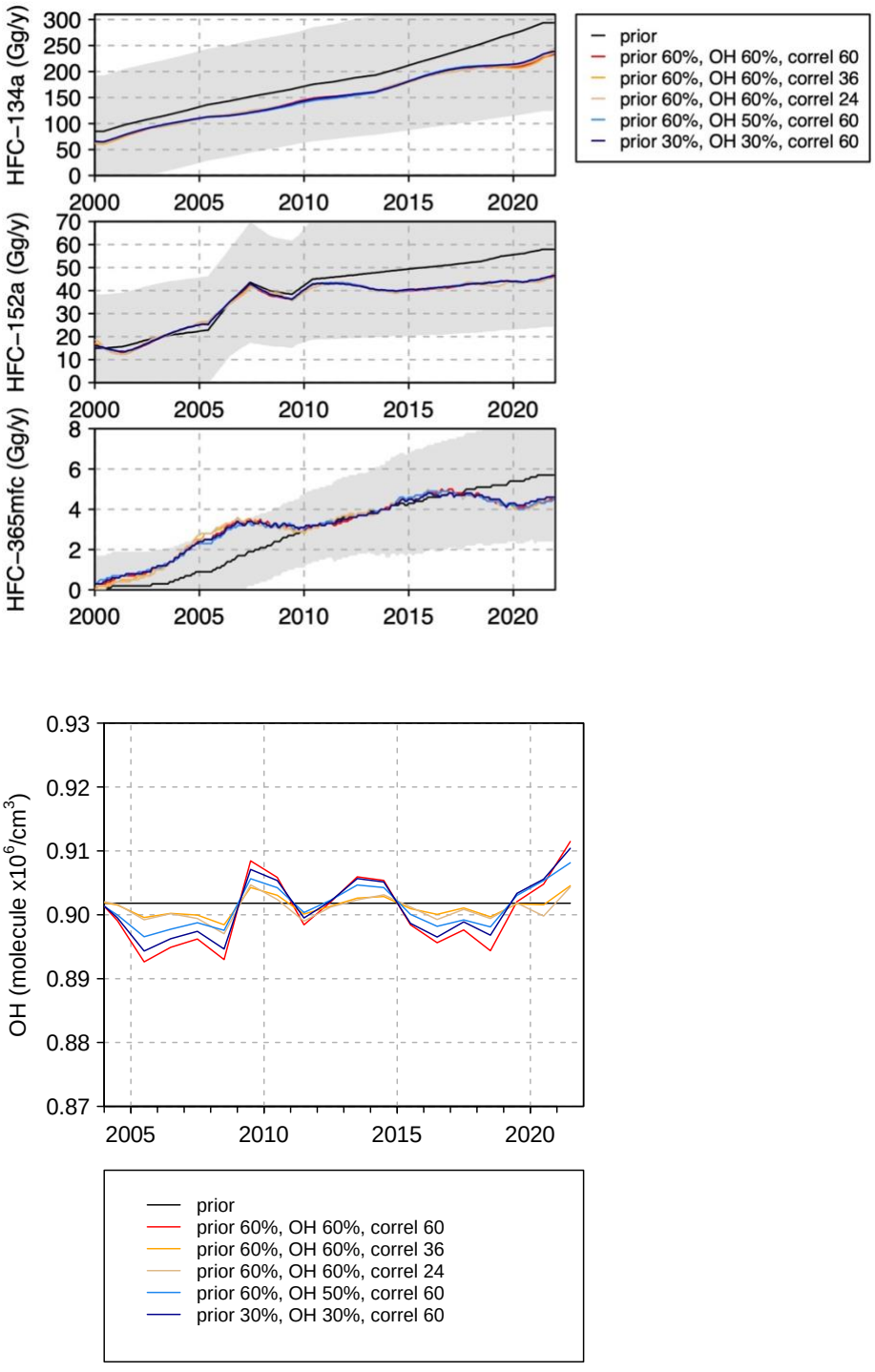

Figure S4: Comparison of the prior, posterior and true OH concentrations in the synthetic data test using HFC-134a, HFC-152a and HFC-365mfc.

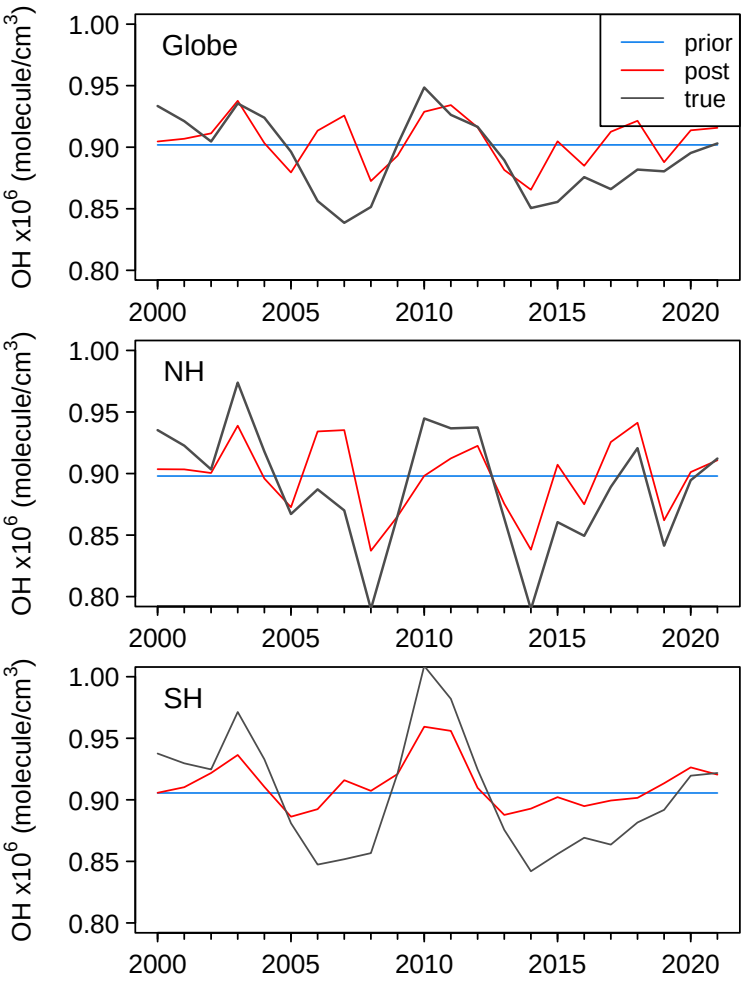

Figure S5: Timeseries of the model-observation error (ppt) for each of the five species used in this study. The black line is the error a priori and the coloured lines are the results from each of the six inversions that included the respective species (see legend).

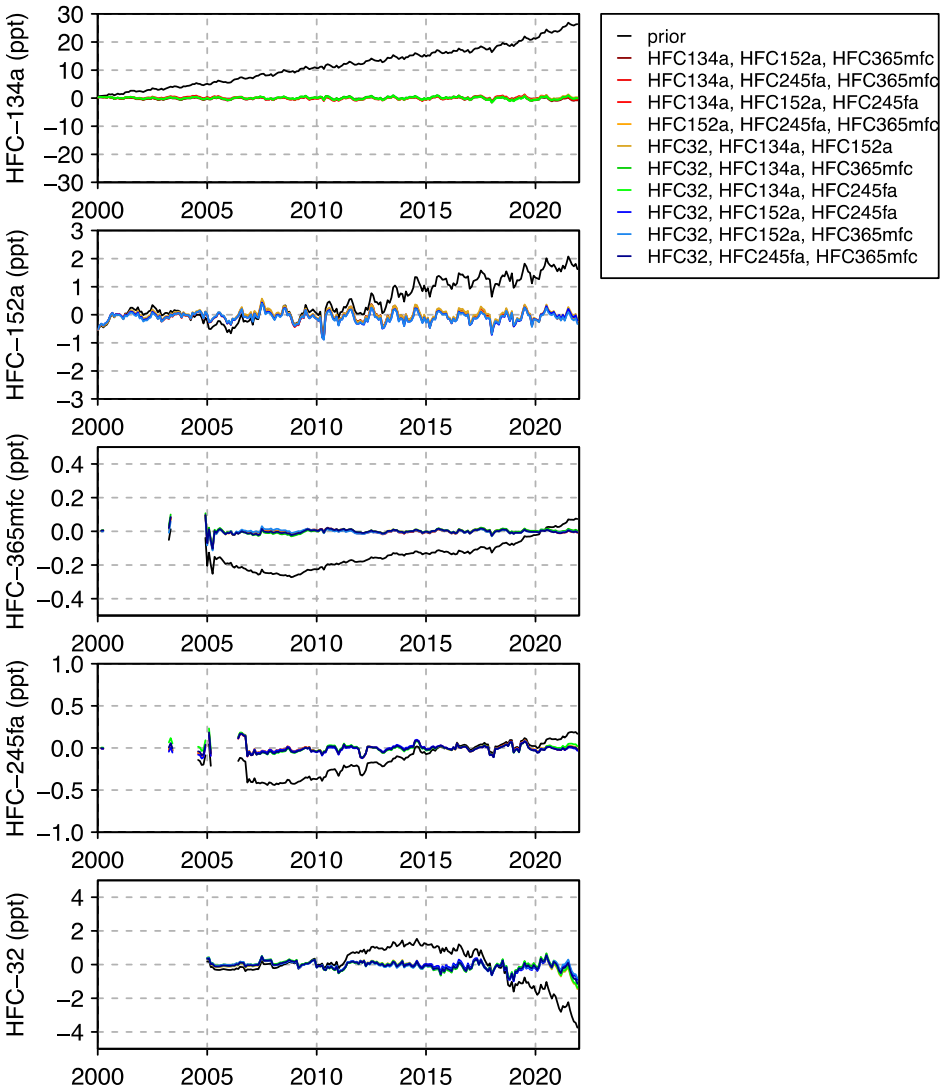

Figure S6: Timeseries of monthly global mean emissions (Gt/y). The black line is the prior with the prior uncertainty indicated by the grey shading. The coloured lines are the posterior emissions from the six inversions that included the respective species (see legend).

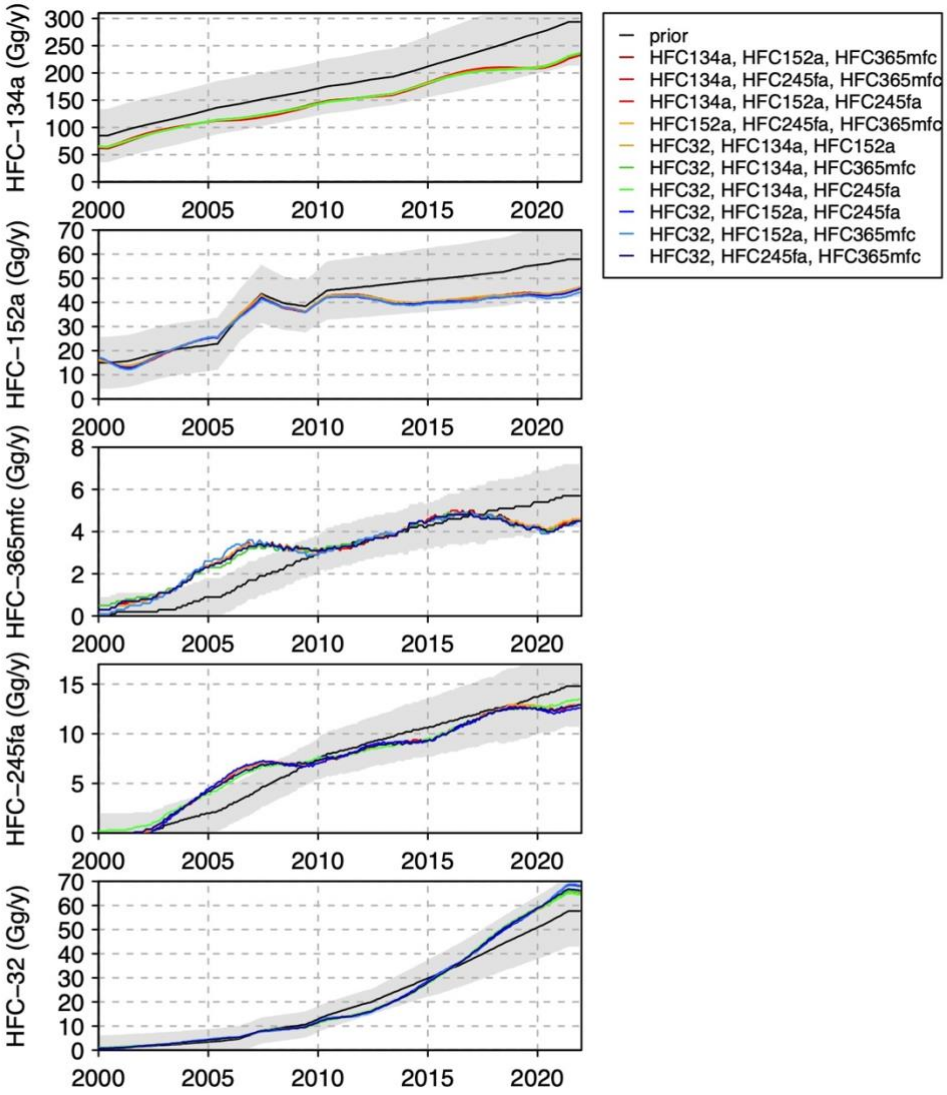

Figure S7. Time series of the global annual mean OH concentration shown for 2004-2021 from all 10 inversions in which NOAA data for HFC-32 and HFC-365mfc were adjusted to match the AGAGE scale.

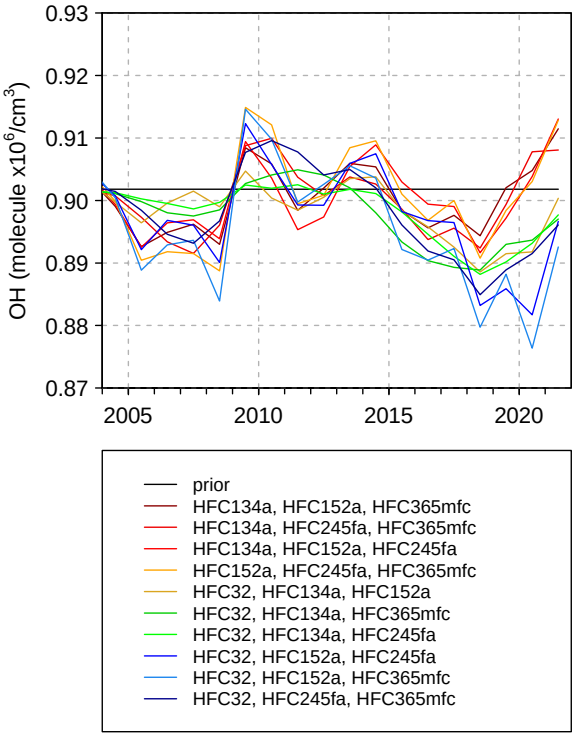

Figure S8. Monthly OH anomaly (%) and MEI smoothed using a spline fit (top panel) and scatter plots of monthly OH anomaly versus MEI using a lag in OH of 6 months (lower left panel) and 9 months (lower right panel).

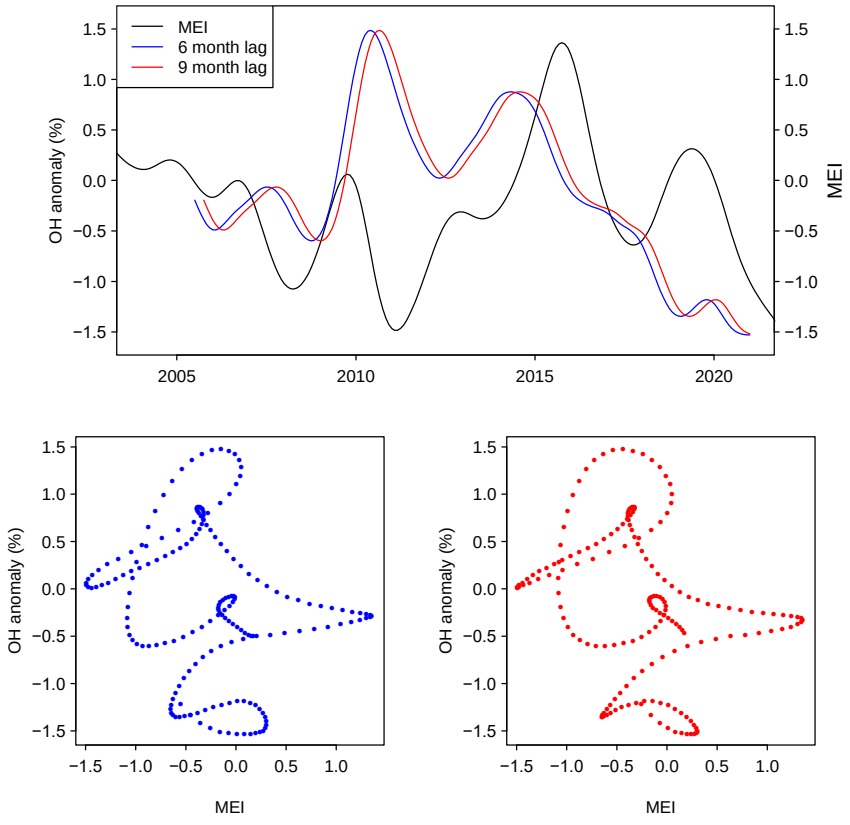

Figure S9. Monthly mean CH_4 mole fractions in each latitudinal box in the lower troposphere calculated as the mean of all sites in each box. These are the observation data that were assimilated in the CH_4 inversions.

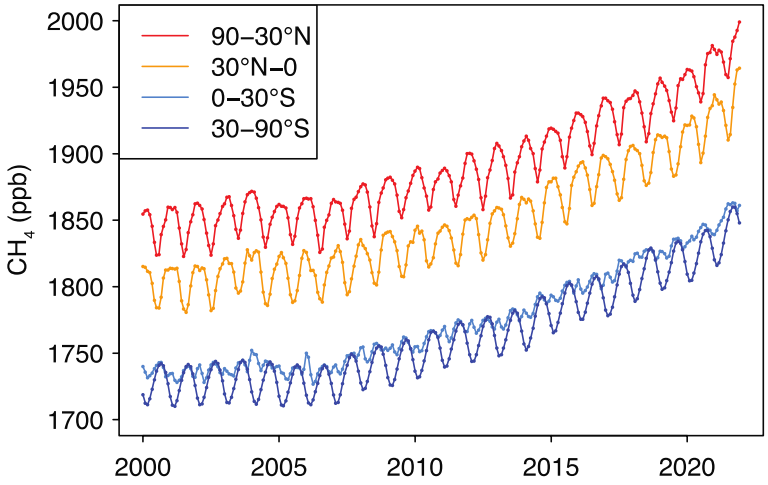

References

Mellouki, A., Téton, S., and Bras, G. L.: Rate constant for the reaction of OH radical with HFC-365mfc (CF3CH2CF2CH3), Geophys Res Lett, https://doi.org/10.1029/94gl03275, 1995.

Orkin, V. L., Huie, R. E., and Kurylo, M. J.: Atmospheric Lifetimes of HFC-143a and HFC-245fa: Flash Photolysis Resonance Fluorescence Measurements of the OH Reaction Rate Constants, J Phys Chem, 100, 8907–8912, https://doi.org/10.1021/jp9601882, 1996.

Wilson, E. W., Hamilton, W. A., Mount, H. R., and DeMore, W. B.: Rate Constants for the Reactions of Hydroxyl Radical with Several Fluoroethers by the Relative Rate Method, J Phys Chem, 111, 1610–1617, https://doi.org/10.1021/jp068355d, 2007.